Energy Proceedings
Vol 41, 2024
ISSN 2004-2965

# Electrochemical Performance of Dual-layer Carbon Electrodes for Aqueous Redox Flow Batteries

Baichen Liu[1], Salvatore De Angelis[1], Vedrana Andersen Dahl[2], Søren Bredmose Simonsen[1], Johan Hjelm[1*]

1 Department of Energy Conversion and Storage, Technical University of Denmark
Building 310, DK-2800 Kgs. Lyngby, Denmark

2 Department of Applied Mathematics and Computer Science, Technical University of Denmark
Building 310, DK-2800 Kgs. Lyngby, Denmark
(*Corresponding Author: johh@dtu.dk)

**ABSTRACT**

Recognizing the urgent need for further cost reduction to drive broad adoption of redox flow batteries, it is critical to improve the reactor performance. Improved performance leads to higher efficiency, potential for a decrease of the stack size, and reduced capital cost. As one of the main contributors to reactor internal resistance, porous electrodes with properly designed structures and optimized physicochemical properties offer a pathway to reduced voltage losses, including kinetic and concentration overpotentials. Recently, carbon cloth electrodes were explored in flow battery applications owing to their bimodal pore size distributions, which opens a potential opportunity for improved mass transport behavior. Although the unique woven structure of cloth provides flexibility in the electrode design, finding an optimal trade-off between abundant electrolyte penetration pathways and a high active surface area is still challenging. In the present study, we investigate a dual-layer electrode configuration to meet the requirements of high active surface area and low mass transport resistance. A carbon cloth was placed close to the flow plate to serve as an electrolyte distributor to ensure efficient mass transport in a lateral flow-through configuration, and a carbon paper sub-layer was placed near the membrane to provide a high density of reaction sites. Overall, the results show that the proposed strategy is an effective way to achieve high electrochemical performance and low pressure drop. It can be regarded as a promising approach for boosting system efficiency.

**Keywords:** woven carbon electrode, mass transport, Lattice-Boltzmann method, symmetric cell, redox flow battery

**NONMENCLATURE**

| | |
|---|---|
| *Abbreviations* | |
| BET | Brunauer-Emmett-Teller |
| CT | Computed Tomography |
| DL | Dual-layer |
| EIS | Electrochemical Impedance Spectroscopy |
| FTFF | Flow-through Flow Field |
| LBM | Lattice Boltzmann Method |
| RFB | Redox Flow Battery |
| SoC | State-of-charge |
| *Symbols* | |
| $k_m$ | Mass Transfer Coefficient |
| $v_e$ | Linear Flow Velocity |

## 1. INTRODUCTION

Redox flow batteries (RFBs) are considered one of the most suitable technologies for medium to large-scale energy storage applications [1]. Such applications are expected to facilitate integration of intermittent renewables, such as wind and solar energy. In recent years, tremendous efforts have been placed in improving battery performance through development of critical battery components, including electrolytes [2], membranes [3], electrodes [4], etc. Increasing the efficiency of the reactors is an important pathway to bringing down the high capital cost of state-of-the-art RFBs [5].

Porous electrodes are core components within the reactor, which provide active reaction sites and electrolyte transport pathways [6]. Popular carbon-fiber porous electrodes adopted in RFBs include carbon felt,

# This is a paper for 15th International Conference on Applied Energy (ICAE2023), Dec. 3-7, 2023, Doha, Qatar.

carbon paper, and carbon cloth [7]. Numerous studies have been conducted to improve the hydrophilicity and increase the active surface area, e.g., by applying different pretreatment approaches [8], pore etching [9], and surface modification [10]. However, it remains a challenge to simultaneously meet the requirements of high active surface area for reduced kinetic resistance and a consistent pore network with appropriate pore sizes for enhanced permeability and mass transport.

To overcome the high pressure drop electrodes with large volumetric specific surface area (high fiber density, e.g., carbon paper), numerous flow field designs on the flow plates used in single-cell test hardware (e.g., serpentine [11], interdigitated [12], etc.) have been developed to enable "flow-by" electrolyte flow over the electrode surface and force convection into the electrode structure to enhance local mass transport [13]. Balancing the interactions between the flow fields and porous electrodes is important to optimize the transport behavior and related losses. Considering the relatively low flexibility of the electrode internal structure, more efforts have been put into optimization of flow fields including geometric channel sizes [14] and flow pathway designs [15] to obtain homogeneous electrolyte distributions and low mass transfer losses. A common geometry in industrial stacks is the use of planar bipolar plates without integrated flow fields. A possible method to enable higher electrolyte flow velocities at a low pressure drop penalty is to use a bimodal pore size distribution in the flow through electrode. Carbon cloths, due to the flexibility of woven pattern designs offers access to bimodal pore size distributions [16], and provide some potential to partially take on the function of a flow field to facilitate electrolyte penetration along the woven direction at low pressure drop.

Due to the presence of the large void and well-defined microstructure, carbon cloth has been shown to be a high-performance electrode with reduced mass transport resistance and pressure drop in a full-cell RFB system [17]. The physical and electrochemical properties of carbon cloth with different woven patterns were compared in both aqueous [18] and non-aqueous [19] RFBs. Although the effectiveness of carbon cloth adoption in RFBs was validated, the local mass transport behavior still needs in-depth investigation. Modeling and simulation work is an effective approach to investigate the fluid dynamics. However, the non-uniform internal structure of carbon cloth adds significant complexity to the simulations using finite element methods. Zhang et al. [20] adopted the computationally inexpensive Lattice Boltzmann Method (LBM) in conjunction with X-ray computed tomography to simulate electrode permeability and velocity profiles in carbon cloth electrodes. The influence of the cloth structure on local mass transport needs further exploration.

Inspired by the periodic woven structure of carbon cloth, we focused on a dual-layer (DL) electrode configuration, where the carbon cloth placed near the flow plates (corresponding to the bipolar plate in a stack) and the carbon paper placed adjacent to the membrane. The carbon cloth serves as a simplified flow field, and the through-plane electrolyte convection can support efficient mass transfer into the carbon paper. It is noted that some double-layer [21][22][23] or triple-layer electrode [24] structures in RFBs were proposed in the literature with the combination of carbon felt and carbon paper. Multi-layer carbon paper electrodes with gradient porosity [25] or multi-segmented carbon felts [26] were also proposed for enhanced battery performance. However, the benefits were relatively limited due to the minor impacts on flow behavior from the uniform electrode structure. Wu et al. [27] proposed a thin-film electrode assembly with combinations of carbon cloth and electrospun fiber mat coupled with different flow fields. Such an electrode assembly proved to be beneficial to improve the energy efficiency under an interdigitated flow field. However, the idea of the carbon cloth to distribute electrolyte in a flow-through configuration still needs to be investigated.

In the present study, two carbon cloths with different woven structures were selected and combined with the carbon paper. The pressure drop and electrochemical performance of the DL configuration were measured. Quantitative analysis for polarization losses was performed using symmetric vanadium flow cells with a flow-through flow field (FTFF). The results showed that the DL configuration is an effective strategy to obtain decreased overall kinetic and mass transport resistances. The overall full-cell overpotential reach ~0.08 V at 100 mA/cm$^2$, a decrease of ~35% and ~17% compared to single-layer carbon cloth and paper, respectively.

## 2. EXPERIMENTAL

### *2.1 Electrode preparation*

Two woven carbon cloth electrodes (AvCarb 1186 HCB and ELAT-H) and a non-woven carbon paper electrode (Freudenberg H23) were investigated in the present study. All electrodes were cut to 5 cm$^2$ squares and thermally treated at 400 $^{o}$C for 24 hours in air to ensure hydrophilicity before assembled into the battery

setup. In this work, AvCarb 1186 and ELAT-H carbon cloth were combined with Freudenberg H23 carbon paper, respectively, referred to as A-FDL and E-FDL electrode assemblies. The three individual electrodes were tested, and their performance contrasted with the two double layer electrode assemblies.

### *2.2 Electrode microstructure characterization*

X-ray computed tomography (CT) was used to capture the internal microstructure of the selected electrodes. The electrode sample after thermal treatment was cut to a cylinder with the diameter of ~1 cm and placed in a sample holder in a ZEISS XRadia 410 Versa.

### *2.3 Flow cell testing*

A single-cell battery reactor with the active area of 5 $cm^2$ (Fuel Cell Technologies) was assembled. A 10 µm thick meta-polybenzimidazole (m-PBI) membrane (Blue World Technologies) was sandwiched between the two electrodes. The compression of all electrodes and electrode combinations was maintained at 20±2%.

A symmetric cell setup was established as shown in Fig. 1. In the present study, we investigated both a negative (i.e., $V^{2+}/V^{3+}$) and positive (i.e., $VO^{2+}/VO_2^+$) vanadium symmetric cell. The original electrolyte (Oxkem) containing 1.6 mol/L vanadium species ($V^{3+}$:$VO^{2+}$:=1:1), 4 mol/L sulphate, and 0.05 mol/L phosphoric acid was pre-charged to 50% state-of-charge (SoC). A Bio-Logic SP-300 potentiostat was used to collect data from electrochemical impedance spectroscopy (EIS) and polarization measurements.

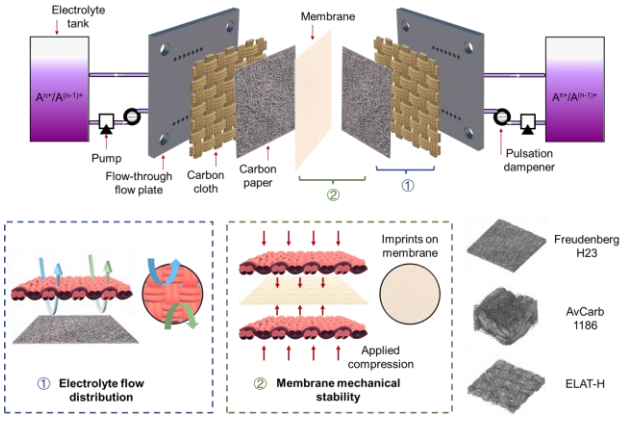


Fig. 1. Design of the dual-layer electrode configurations in a symmetric cell

For mass transfer coefficient ($k_m$) measurements, the original vanadium electrolytes were first diluted to 0.1 mol/L ($V^{3+}$:$VO^{2+}$:=1:1) using 2 mol/L $H_2SO_4$ to maintain the sulphate concentration, and then pre-charged to 50% SoC. Linear sweep voltammetry was performed from 0 V until the current reached a plateau, which was regarded as the limiting current to determine the $k_m$.

### *2.4 Pressure drop measurement*

Electrode permeability was estimated through pressure drop measurement. Two pressure sensors (Grundfos Direct Sensors, RPS 0-2.5) were connected at the inlet and outlet of the battery on one side to collect the pressure signal. The working fluid in pressure-drop measurements was deionized water (18 MΩ).

## 3. LBM SIMULATION

To better understand the flow distribution in the dual-layer electrode configurations, qualitative flow simulations using LBM were performed in the open-source library Palabos [28] using 16 nodes with 8 processors per node. The image data (301x301x100 voxels) of dual-layer electrode configurations were constructed digitally through separate datasets of carbon cloth and carbon paper obtained through X-ray CT after segmentation. A pressure gradient was imposed between the two sides along the cross-section of the electrodes to represent lateral flow in FT-FF under practical battery condition. We note that the present results are only qualitative, and more effort is needed to carefully match the simulations' boundary conditions with real-world experiments. Furthermore, a bigger volume should be simulated to avoid edge effects and be more representative of the real device. More quantitative simulations will be performed in a future study.

## 4. RESULTS AND DISCUSSION

### *4.1 Pressure drop tests*

Fig. 2(a) shows the pressure-drop results of the five electrode configurations in a FTFF single-cell setup. The non-linear Darcy-Forchheimer equation was used for fitting to the experimental pressure drop results. The carbon paper exhibits extremely high pressure drop due to the high fiber density and low thickness. The permeability of the carbon paper is $3.2\times10^{-11}$ $m^2$, which is lower than that of the carbon cloth ($11.1\times10^{-11}$ $m^2$ for AvCarb 1186 and $25.3\times10^{-11}$ $m^2$ for ELAT-H).

However, when coupled with a single layer of carbon cloth near the flow plate, the pressure drop of the DL configurations are greatly reduced. The best fit permeability of A-FDL and E-FDL was $10.7\times10^{-11}$ $m^2$ and $14.9\times10^{-11}$ $m^2$, respectively. We found that the

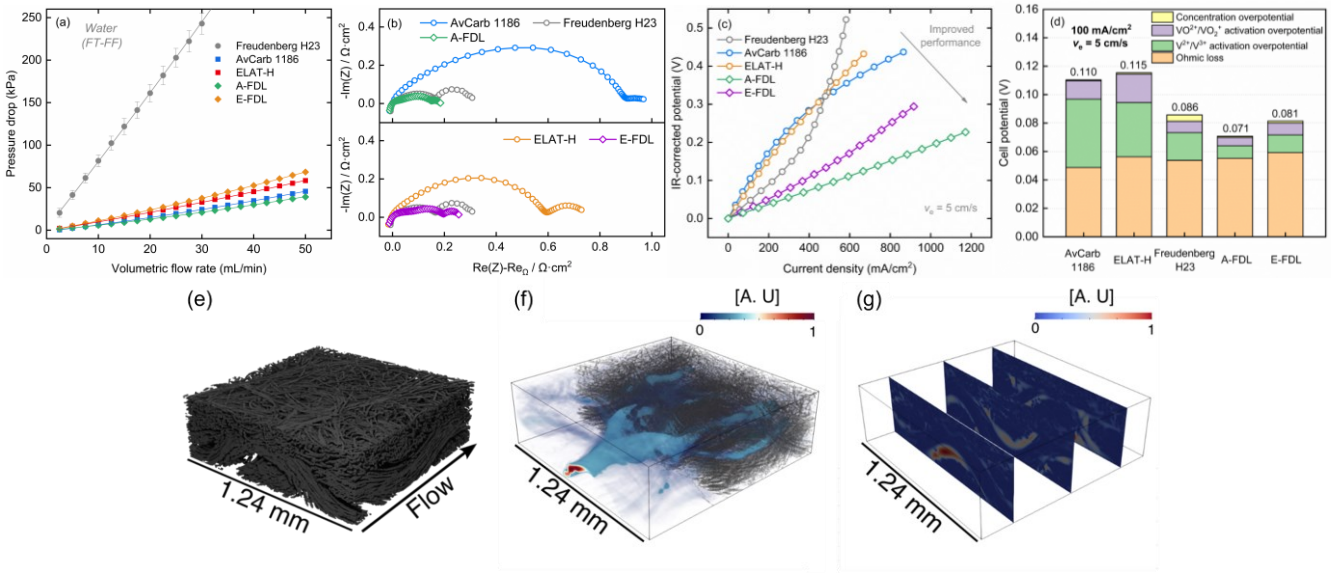


Fig. 2. Comparison of the (a) pressure drop, (b) EIS performance with 1.6 M $V^{2+}/V^{3+}$ in symmetric cells (c) iR-corrected polarization with 1.6 M $V^{2+}/V^{3+}$ in symmetric cells, (d) column analysis of cell potential. LBM flow distributions of the E-FDL is presented: (e) 3D rendering of the constructed volume used for the flow simulations, (f) Volume rendering of the normalized velocity magnitude, (g) 2D slices of the normalized velocity magnitude field.

permeability of A-FDL is similar to that of the single-layer AvCarb 1186. This indicates that within the A-FDL configuration, most electrolyte still flows through the carbon cloth layer, probably due to electrode thickness and the relatively large voids at the intersection between fiber bundles.

### *4.2 Symmetrical cell testing*

Symmetrical cell measurements in both positive (i.e., $VO^{2+}/VO_2^+$) and negative (i.e., $V^{2+}/V^{3+}$) electrolytes was conducted. Here we only present the results from the negolyte cell tests. From the EIS measurements at the same flow velocity ($v_e$=5 cm/s) in Fig. 2(b), we find that the carbon cloth electrodes exhibit a low mass transfer impedance. However, the performance is limited by high kinetic resistance due to the low active specific surface area (BET surface area: 0.6 and 1.8 $m^2/g$ for AvCarb 1186 and ELAT-H, respectively), especially for the more sluggish redox couple (i.e., $V^{2+}/V^{3+}$). In contrast, the carbon paper possesses high surface area after thermal treatment (BET surface area: 53.6 $m^2/g$), which significantly contributes to the reduced kinetic resistance. However, the mass transport properties of carbon paper electrodes are relatively poor, yielding high pressure drop and high mass transfer resistance. For the two DL configurations, the overall resistances are both reduced compared to the carbon paper. Specifically, the total resistances of kinetic and mass transport are reduced by ~40% and ~17% for A-FDL and E-FDL, respectively, compared to that of carbon paper.

Fig. 2(c) shows the iR-corrected polarization results for symmetric cells with $V^{2+}/V^{3+}$ redox couples. Similar to the EIS results, the DL configurations show lower overpotentials compared to the single-layer electrodes. A-FDL shows superior electrochemical performance with <0.1 V voltage loss at a current density of 500 $mA/cm^2$. This is consistent with the low kinetic and mass transfer impedances observed for this dual layer electrode (A-FDL). The overpotential of carbon paper increases rapidly when >400 $mA/cm^2$, which exhibits characteristics of mass transport limitation.

### *4.3 Full-cell polarization analysis*

To obtain the mass transfer coefficient of each electrode configuration, limiting current density measurements are conducted at different flow rates. km can subsequently be fitted as a function of flow velocity and the observed limiting current at different ve. After obtaining km, the concentration overpotential can be calculated assuming 0 concentration of active species at the fiber surface under limiting current conditions. Hereby, full-cell polarization analysis is conducted on the basis of measured mass transfer coefficient, and ohmic losses from high-frequency region of EIS after removal inductance. The activation overpotentials for $V^{2+}/V^{3+}$ and $VO^{2+}/VO_2^+$ are calculated by subtracting concentration overpotentials and ohmic losses from the overall polarizations. The results at a current density of 100 $mA/cm^2$ and at ve=5 cm/s are shown in Fig. 2(d). It was found that the high performance of DL configurations

compared to the other three single-layer electrode mainly comes from reduced activation overpotential of $V^{2+}/V^{3+}$, and a low concentration overpotential. Although the ohmic loss is slightly increased due to the introduction of an additional electrode layer, the full-cell overall overpotential is still reduced by ~35% and ~30% for A-FDL and E-FDL, respectively, compared to the single-layer carbon cloth.

### *4.4 LBM flow distributions*

To better understand the flow distribution in the DL electrode configuration, qualitative flow simulations using the LBM were conducted. The volume rendering of the velocity magnitude in Fig. 2(f) qualitatively shows that the flow velocity is greatest in the large channels of the carbon cloth while it is much lower in the carbon paper and within the fiber bundles of the cloth. Fig. 2(g) shows different slices of the normalized velocity magnitude along the flow direction. In all slices, the maximum velocity is observed in the middle of the cloth's channels, between the different bundles. The presented results are only qualitative. More effort is needed to carefully match the boundary conditions with practical experiments. Furthermore, a bigger volume should be simulated to avoid edge effects and be more representative of the real device. More quantitative simulations will be performed in a future study.

## 5. CONCLUSIONS

The present study investigated a dual-layer electrode configuration with the combination of carbon cloth and carbon paper. We show that a carbon cloth with bimodal pore size distribution can effectively function as a flow field in combination with a carbon paper electrode. The high permeability of the carbon cloth results in low pressure drop at a high linear flow velocity, effectively reducing the mass transfer losses, while the high fiber density of the carbon paper results in low kinetic losses. Overall, the proposed strategy has been proven to be effective to achieve low pressure drop and high full-cell electrochemical performance with the benefits mainly from a decrease of the total mass transfer losses and the kinetic overpotential of the $V^{2+}/V^{3+}$ redox couple. This type of dual-layer electrode configuration could potentially be employed to significantly increase the performance of conventional flow-through stack designs.

## DECLARATION OF CONFLICT OF INTEREST

The authors declare that they have no known competing financial interests or personal relationships that could have appeared to influence the work reported in this paper. All authors read and approved the final manuscript.


## ACKNOWLEDGEMENT

This work was supported by EUDP through RED-BATS (project no 64020-2095) and by Innovation Fund Denmark through DanFlow (file no. 9090-00059B).


## REFERENCE


[1] M. Rahman, A. Oni, E. Gemechu, A. Kumar. Assessment of energy storage technologies: A review. Energy Conversion and Management, 223, 113295 (2020).

[2] K. Lin, Q. Chen, M. Gerhardt, L. Tong, S. Kim, L. Eisenach, A. Valle, D. Hardee, R. Gordon, M. Aziz, M. Marsha. Alkaline quinone flow battery. Science, 349, 1529−1532 (2015).

[3] Z. Yuan, Y. Duan, H. Zhang, X. Li, H. Zhang, I. Vankelecomd. Advanced porous membranes with ultra-high selectivity and stability for vanadium flow batteries. Energy & Environmental Science, 9, 441−447 (2016).

[4] C. Wan, R. Jacquemond, Y. Chiang, K. Nijmeijer, F. Brushett, A. Forner-Cuenca. Non-Solvent induced phase separation enables designer redox flow battery Electrodes. Advanced Materials, 33, 2006716 (2021).

[5] J. Noack, L. Wietschel, N. Roznyatovskaya, K. Pinkwart, J. Tübke. Techno-economic modeling and analysis of redox flow battery systems. Energies, 9, 627 (2016).

[6] R. Wang, Y. Li. Carbon electrodes improving electrochemical activity and enhancing mass and charge transports in aqueous flow battery: Status and perspective. Energy Storage Materials, 31, 230−251 (2020).

[7] A. Forner-Cuenca, F. Brushett. Engineering porous electrodes for next-generation redox flow batteries: recent progress and opportunities. Current Opinion in Electrochemistry, 18, 113-122 (2019).

[8] K. Greco, A. Forner-Cuenca, A. Mularczyk, J. Eller, F. Brushett. Elucidating the nuanced effects of thermal pretreatment on carbon paper electrodes for vanadium redox flow batteries. ACS Applied Materials & Interface, 10, 44430−44442 (2018).

[9] X. Zhou, T. Zhao, Y. Zeng, L. An, L. Wei. A highly permeable and enhanced surface area carbon-cloth electrode for vanadium redox flow batteries. Journal of Power Sources, 329, 247−254 (2016).

[10] Y. Zhao, L. Yu, X. Qiu, J. Xi. Carbon layer-confined sphere/fiber hierarchical electrodes for efficient and

durable vanadium flow batteries. Journal of Power Sources, 402, 453–459 (2018).
[11] Q. Xu, T. Zhao, P. Leung. Numerical investigations of flow field designs for vanadium redox flow batteries. Applied Energy, 105, 47–56 (2013).
[12] Y. Zhang, F. Li, F. Lu, X. Zhou, Y. Yuan, X. Cao, B. Xiang. A hierarchical interdigitated flow field design for scale-up of high-performance redox flow batteries. Applied Energy, 238, 435–441 (2019).
[13] X. Ke, J. Prahl, J. Alexander, J. Wainright, T. Zawodzinski, R. Savinell. Rechargeable redox flow batteries: flow fields, stacks and design considerations. Chemical Society Reviews, 47, 8721–8743 (2018).
[14] R. Gundlapalli, S. Jayanti. Effect of channel dimensions of serpentine flow fields on the performance of a vanadium redox flow battery. Journal of Energy Storage, 23, 148–158 (2019).
[15] V. Muñoz-Perales, M. Heijden, P. García-Salaberri, M. Vera, A. Forner-Cuenca. Engineering lung-inspired flow field geometries for electrochemical flow cells with stereolithography 3D printing. ACS Sustainable Chemistry & Engineering, (2023).
[16] A. Forner-Cuenca, E. Penn, A. Oliveira, F. Brushett. Exploring the role of electrode microstructure on the performance of non-aqueous redox flow batteries. Journal of The Electrochemical Society, 166, A2230–A2241 (2019).
[17] M. León, L. Castañeda, A. Márquez, F. Walsh, J. Nava. Review—carbon cloth as a versatile electrode: manufacture, properties, reaction environment, and applications. Journal of The Electrochemical Society, 169, 053503 (2022).
[18] A. Wong, M. Aziz. Method for Comparing porous carbon electrode performance in redox flow batteries. Journal of The Electrochemical Society, 167, 110542 (2020).
[19] K. Tenny, A. Forner-Cuenca, Y. Chiang, F. Brushett. Comparing physical and electrochemical properties of different weave patterns for carbon cloth electrodes in redox flow batteries. Journal of Electrochemical Energy Conversion and Storage, 17, 041010 (2020).
[20] D. Zhang, A. Forner-Cuenca, O. Taiwo, V. Yufit, F. Brushett, N. Brandon, S. Gu, Q. Cai. Understanding the role of the porous electrode microstructure in redox flow battery performance using an experimentally validated 3D pore-scale lattice Boltzmann model. Journal of Power Sources, 447, 227249 (2020).
[21] C. Zeng, S. Kim, Y. Chen, Y. Fu, J. Bao, Z. Xu, W. Wang. Characterization of electrochemical behavior for aqueous organic redox flow batteries. Journal of The Electrochemical Society, 169, 120527 (2022).
[22] M. Manahan, Q. Liu, M. Gross, M. Mench. Carbon nanoporous layer for reaction location management and performance enhancement in all-vanadium redox flow batteries. Journal of Power Sources, 222, 498–502 (2013).
[23] W. Chen, J. Kang, Q. Shu, Y. Zhang. Analysis of storage capacity and energy conversion on the performance of gradient and double-layered porous electrode in all vanadium redox flow batteries. Energy, 180, 341–355 (2019).
[24] M. Raja, H. Khan, S. Sankarasubramanian, D. Sonawat, V. Ramani, K. Ramanujam. Binder-free thin graphite fiber mat sandwich electrode architectures for energy-efficient vanadium redox flow batteries. Catalysis Today, 370, 181–188 (2021).
[25] H. Jiang, B. Zhang, J. Sun, X. Fan, W. Shyy, T. Zhao. A gradient porous electrode with balanced transport properties and active surface areas for vanadium redox flow batteries. Journal of Power Sources, 440, 227159 (2019).
[26] R. Cheng, J. Xu, J. Zhang, P. Leung, Q. Ma, H. Su, W. Yang, Q. Xu. Facile segmented graphite felt electrode for iron-vanadium redox flow batteries with deep eutectic solvent (DES) electrolyte. Journal of Power Sources, 483, 229200 (2021).
[27] Q. Wu, Y. Lv, L. Lin, X. Zhang, Y. Liu, X. Zhou. An improved thin-film electrode for vanadium redox flow batteries enabled by a dual layered structure. Journal of Power Sources, 410–411, 152–161 (2019).
[28] J. Latt, O. Malaspinas, D. Kontaxakis, A. Parmigiani, D. Lagrava, F. Brogi, M. Belgacem, Y. Thorimbert, S. Leclaire, S. Li, F. Marson, J. Lemus, C. Kotsalos, R. Conradin, C. Coreixas, R. Petkantchin, F. Raynaud, J. Beny, B. Chopard. Palabos: Parallel Lattice Boltzmann Solver. Computers & Mathematics with Applications, 81, 334–350 (2021).